Controlling the polymorphism and topology transformation in porphyrinic zirconium metal-organic frameworks via mechanochemistry

Bahar Karadeniz,[†] Dijana Žilić,[†] Igor Huskić,[‡] Luzia S. Germann,[¥,‡] Athena M. Fidelli,[‡] Senada Muratović,[†] Ivor Lončarić,[†] Martin Etter,[∥] Robert. E. Dinnebier,[¥] Dajana Barišić,[†] Nikola Cindro,[⁋] Timur Islamoglu,[§] Omar K. Farha,[§] Tomislav Friščić,[‡,†] Krunoslav Užarević[†*]

† Ruđer Bošković Institute, 10000 Zagreb, Croatia.

‡ McGill University, Montreal, QC H3A 0B8, Canada.

¥ Max Planck Institute for Solid-State Research, 70569 Stuttgart, Germany.

§ Northwestern University, Evanston, IL 60208, USA.

∥ Deutsches-Elektronen Synchrotron, DESY, 22607 Hamburg, Germany.

⁋ Faculty of Science, University of Zagreb, 10000 Zagreb, Croatia.

Supporting Information Placeholder

ABSTRACT: Tetratopic porphyrin-based MOFs represent a particularly interesting subclass of zirconium MOFs due to the occurrence of several divergent topologies. The control over the target topology is a demanding task and reports often show products containing phase contamination. We demonstrate how mechanochemistry can be exploited for controlling the polymorphism in 12-coordinated porphyrinic zirconium MOFs, gaining pure hexagonal (shp) PCN-223 and cubic (ftw) MOF-525 phases in 20-60 minutes of milling. The reactions are mainly governed by the milling additives and the zirconium precursor. In situ monitoring by synchrotron powder X-ray diffraction (PXRD) revealed that specific reaction conditions resulted in the formation of MOF-525 as an intermediate, which rapidly converted to PCN-223 upon milling. Electron spin resonance (ESR) measurements revealed significant differences between the spectra of paramagnetic centers in two polymorphs, showing a potential of polymorphic Zr-MOFs as tunable supports in spintronics applications.

Metal-organic frameworks (MOFs) received wide attention due to their potential for applications in gas storage[1–3] and separation,[4,5] catalysis,[6,7] drug delivery,[8] light-harvesting,[9,10] and destruction of harmful compounds such as chemical warfare agents.[11] Their superior performance stems from the existence of pores and channels enabling easy access of substrates to the active sites inside the MOF crystals. The use of MOFs as heterogeneous catalysts and catalysts supports is broadened after the introduction of Zr-MOFs based on zirconium $[Zr_6(OH)_4O_4]^{12+}$ oxo-clusters and carboxylate linkers,[12] which provided a way to overcome challenges related to the robustness of MOFs under humid, acidic or basic media.[11,13] They also drew significant interest in an area of MOF-polymorphism. Zr-MOFs based on tetratopic *tetrakis*(4-carboxyphenyl) porphyrin (TCPP) linkers displayed unprecedented flexibility in topological ordering. They are known to exist in six different topologies,[14,15–22] 12-connected cubic *ftw* (MOF-525)[21] and hexagonal *shp* (PCN-223),[16] 8-connected *sqc* (PCN-225),[17] *csq* (PCN-222/MOF-545),[19,21] and *scu* (NU-902),[15] and 6-connected *she* (PCN-224).[20] Recent studies have been focused on establishing different reaction parameters (i.e., p*K*a of modulator, solvent, or temperature) for gaining control over the preparation of a specific target topology, but it proved as a rather demanding task since these polymorphs often crystallize in mixtures.[23–26] Control in polymorph formation is fundamentally interesting for defining parameters that would enable the preparation of different MOFs from identical constituents. It is also expected to have a clear impact on their applicability, as it was recently discovered that the difference in Zr-MOF topologies significantly affects their catalytic activity and gas adsorption properties.[15]

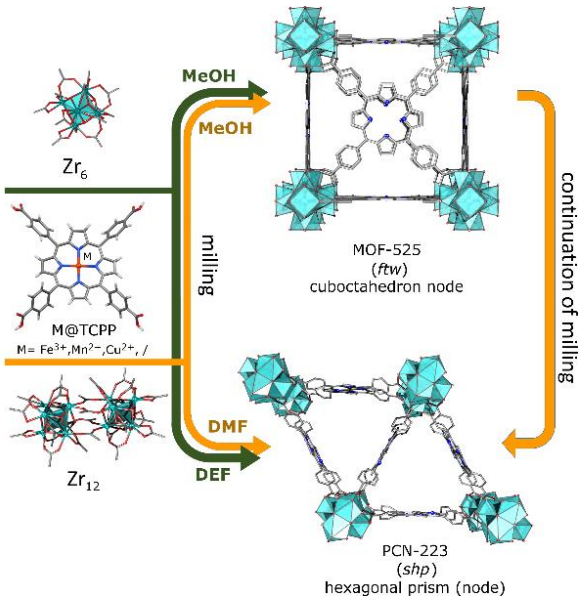

Figure 1. Mechanochemical reactions of M@TCPP and different zirconium precursors for controllable preparation of MOF-525 or PCN-223.

We demonstrate here a mechanochemical approach[27–32] for controllable, clean, and rapid synthesis of phase-pure porphyrinic zirconium MOF polymorphs, cubic MOF-525 (*ftw* topology), and hexagonal PCN-223 (*shp* topology). We evaluated the influence of the TCPP type, starting zirconium oxo-clusters, and liquid additives on the outcome of milling reactions (Figure 1). I*n situ* monitoring by high-energy PXRD[33–35] at the PETRA III beamline P02.1 Deutsches-Elektronen Synchrotron (DESY) revealed that the majority of the reactions were directly producing either MOF-525 or PCN-223. However, it also revealed that specific reaction conditions induce the fast formation and subsequent transformation of MOF-525 to PCN-223: the first example of such behavior reported for Zr-MOFs (Figure 1). Different internal ordering single Fe(III), Cu(II), or Mn(II) cations in TCPP linkers in polymorphic *ftw* and *shp* MOFs showed a profound effect on their ESR spectra.

Mechanochemical ball-milling has been demonstrated as an efficient method for the preparation of different relevant MOFs, including single-[36,37] and mixed-metal MOF-74 materials,[38] MOF-5,[39] HKUST-1,[40] ZIF-8,[33] Al-fumarate,[28] and several topologically novel MOFs not accessible from solution.[33,40,41] Also, high-quality *fcu*- and *scu*-Zr-MOFs were prepared by mechanochemical procedures,[29,42–44] which allowed for the use of green additives in mechanochemical processing. Mechanochemistry has previously been successfully applied for polymorphism control in co-crystals,[45,46] and discrete[47] and extended coordination compounds.[33,48–50]

The liquid-assisted grinding (LAG)[51] experiments were performed by placing the Zr_6 or Zr_{12} oxo-cluster precursor and TCPP into separate halves of a polytetrafluoroethylene (PTFE) vessel, together with two stainless steel balls (1.4 g each) and a chosen liquid additive ($\eta = 0.65$ µL/mg). The reaction mixture was milled by IST-500 mixer mill (InSolido Technologies, Croatia) operating at 25 Hz (Supporting Information (SI)). We tested three zirconium-based oxo-precursors, *i.e.* Zr_6-methacrylate cluster ($(Zr_6(OH)_4O_4(H_2C{=}C(CH_3)COO)_{12}$, Zr_6-benzoate ($Zr_6(OH)_4(O)_4(C_6H_5COO)_{12}$), and dodecahedral Zr_{12}-acetate ($Zr_{12}O_8(OH)_8(CH_3COO)_{24}$) cluster. Zr_{12}-acetate precursor, built from two $Zr_6(OH)_4O_4$ subunits (Figure 1), was used for mechanochemical preparation of various Zr-MOFs, both in small scale[43] and continuous flow processing.[42] We tested here non-metallated TCPP, and three metallated TCPP derivatives containing a single Cu^{2+}, Mn^{2+}, or Fe^{3+} cation in a porphyrin ring (Cu@TCPP, Mn@TCPP, and Fe@TCPP, respectively).

We started with Zr_6-benzoate cluster precursor. *In situ* monitoring of LAG(*N*,*N*-dimethylformamide, DMF) of Fe@TCPP and Zr_6-benzoate by synchrotron PXRD[35,52] revealed the fast and direct formation of MOF-525, completing upon 30 minutes milling (Figure 2a). The Bragg reflections corresponding to MOF-525 remained constant after 90 minutes milling, and the product is bench stable for months. MOF-525 was the only phase formed from Zr_6-benzoate precursor regardless of the additive used in LAG (SI).

In situ monitoring of the LAG(methanol, MeOH) of Zr_6-methacrylate and Fe@TCPP (Figure 2b-d) revealed the fast formation of MOF-525 after milling for 4 minutes, with reaction reaching completion before the 30 minutes mark. Switching to acetone additive resulted in further acceleration of the reaction, possibly due to the partial dissolution of reactants. MOF-525 starts forming in the first minute of milling, and the reaction was completed within 10 minutes. The formation of MOF-525 in LAG(DMF) was much slower. PCN-223 was yielded exclusively in LAG reaction using *N*,*N*-diethylformamide (DEF) additive, and after 90-180 minutes of milling (Figure S10).

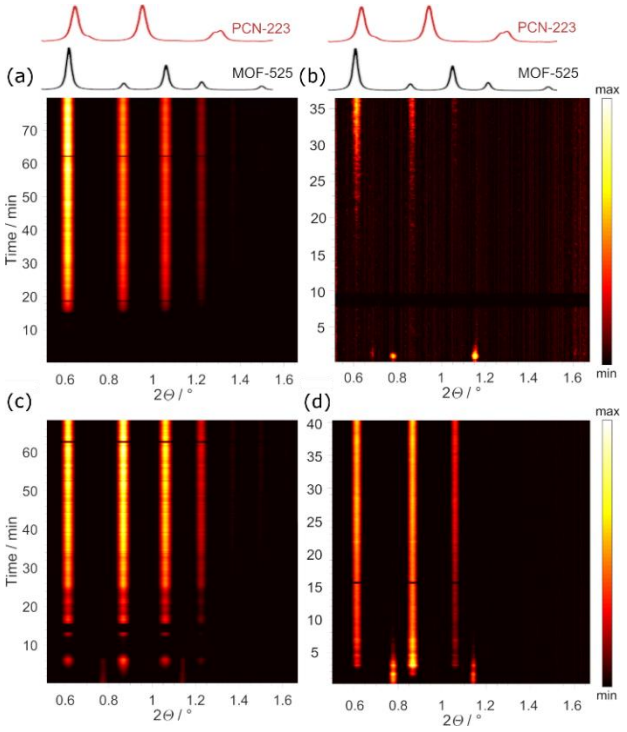

Figure 2. *In situ* PXRD monitoring[34] (10 seconds time-resolution; λ = 0.207 Å) of LAG of Fe@TCPP with a) Zr_6-benzoate using DMF, and Zr_6-methacrylate using b) DMF, c) MeOH, and d) acetone additives. Calculated PXRD patterns of MOF-525[21] and PCN-223[16] are shown above. The variation in intensities at the 5-15 minutes in c) is an artifact of the collection as the sample adhered to the vessel before the released liquids were included in the pores of the formed MOF.[52,53]

In all monitored LAG reactions involving Zr_6 precursors, we have observed the direct formation of MOF-525, which has been previously suggested as a kinetic phase in 12-coordinated porphyrinic Zr-MOFs.[23,24] The first proof of the thermodynamic relation between MOF-525 and PCN-223 has been observed during the mechanochemical reaction of Mn@TCPP and Zr_{12} cluster. In situ monitoring of the LAG(MeOH) of Mn@TCPP and Zr_{12}-acetate (Figure 3a), combined with the sequential Pawley refinement[54] (Figure 3c), where the X-ray reflection intensities are treated as structure-independent parameters, revealed how the formation of MOF-525, after fast initiation, slows significantly when the PCN-223 phase starts to form (around 20-minute mark). Both processes proceed concomitantly for the next 10 minutes, before the Bragg peaks of MOF-525 start to diminish and PCN-223 grows as an exclusive phase, to be finished after 70 minutes milling. The same transformation has been established ex situ for Cu@TCPP, and Fe@TCPP, Figure S16, confirming MOF-525 to be a kinetic polymorph. LAG(DMF) led to slower direct formation of MOF PCN-223 (Figure 3b and d). To compare these results to the previously reported polymorphic pillared MOFs or zeolitic imidazolate frameworks (ZIFs), where the reactions were governed by templation,[48] the volume[52] or acidity[33] of the additive, we reduced the volume of the additive, added additional milling balls for higher-energy milling, or added acetic acid to LAG process, respectively . In all cases, the product was MOF-525 (Figure S18). Thus, we can conclude that the additives govern the observed selectivity, with DEF and DMF governing reactions towards PCN-223. This may be related to DEF or DMF coordinating onto the Zr_6 cluster, forming stable clusters such as 16-coordinated $[Zr_6O_4(OH)_4(CH_2C(CH_3)COO)_{12}(DMF)_4]$, which formed during

LAG(DMF) and hindered mechanochemical preparation of UiO-67.[43]

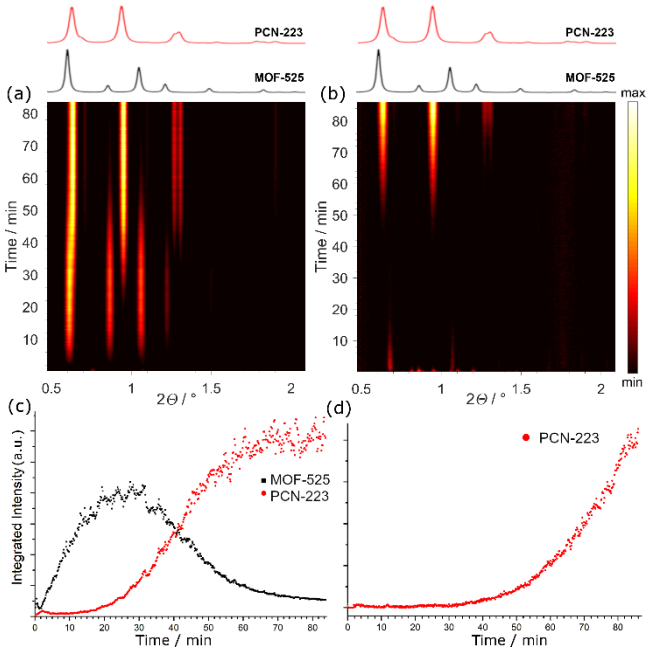

Figure 3. In situ PXRD monitoring (λ = 0.207 Å) of (a) LAG (MeOH) reaction of Mn@TCPP and Zr_{12}-acetate, and (b) LAG(DMF). (d) Change in the integrated peak intensities of MOF-525 ((111) reflection at 1.05 °*2θ*) and PCN-223 ((101) reflection at 0.95 °*2θ*) over time in (c) LAG(MeOH) and (d) LAG(DMF) obtained through sequential Pawley refinement.[54]

The solid-state transformation of MOF-525 to PCN-223 involves significant rearrangements in the crystal structure, the geometry of TCPP, and cluster (Figure 4). The energetic requirements in slurry transformation are demanding; 7 days of stirring a mixture of MOF-525, PCN-224, and PCN-222, at 145 °C was not sufficient to complete the transformation to the thermodynamic phase.[23] It is thus even more interesting to have the full transformation of MOF-525 to PCN-223 in less than 30 minutes of moderate-energy milling. To investigate this further, we attempted to induce the transformation of the isolated and purified MOF-525. Neat grinding of the guest-free MOF-525material led to amorphization of the sample, and the series of LAG and aging experiments did not succeed in transformation (Figures S19-S20). This observation suggest that the energy barrier for the transformation might be too high for our milling setup.[55] Thus, the facile transformation observed during the MOF-525 formation is likely due to a combination of basic and mobile acetate ligands,[24] and the plastic deformations and partially-coordinated clusters occurring during the formation of MOF-525 nuclei, that are still sufficiently disordered and flexible to transform to PCN-223.

Density functional theory calculations confirm the higher stability of PCN-223. We obtained the difference in energy of 1620 kJ/mol[56] between PCN-223 and MOF-525 polymorphs with Cu@TCPP using PBE+D3(BJ) functional.[57–59] Most of this substantial energy difference comes from more negative electrostatic energy in PCN-223 that is more densely packed compared to MOF-525. To attempt decoupling the role of conformation vs. density differences, we compared the energy of the two structures when the volume of PCN-223 is enlarged to match the density of MOF-525. The difference in energy drops to 900 kJ/mol, highlighting the importance of both the different crystal packing and conformational changes (detailed discussion in SI).

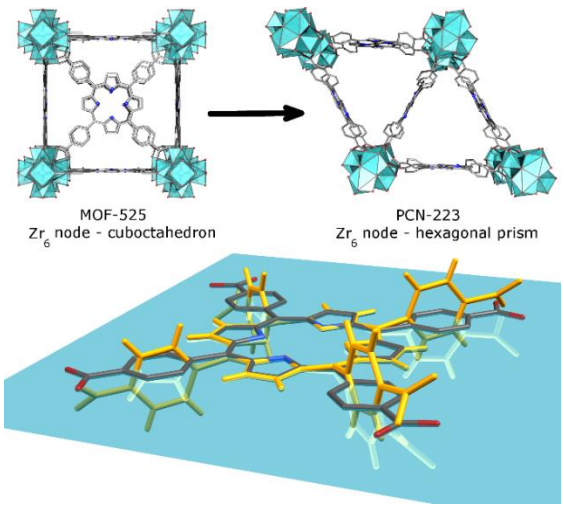

Figure 4. MOF-525 and PCN-223 have different Zr-nodes and 3-D structures. TCPP in MOF-525 is planar, and in PCN-223 (orange molecule) the peripheral phenyls are rotated for almost 90°.

The porosity of products has been established by nitrogen adsorption experiment at 77 K. The established Brunauer-Emmett Teller (BET, SI) surface area values of PCN-223 are in the range of 1340-1500 m^2/g (literature: 1600 m^2/g)[16] and for MOF-525 are in the range of 1740-1870 m^2/g (literature: up to 2620 m^2/g).[21] The samples, after the treatment in acidic DMF solution, thermal activation, and nitrogen sorption remained highly crystalline. The thermogravimetric analysis confirmed thermal behavior similar to their solution-prepared counterparts (Figures S30-S33).

The distance of two nearest metal cations in the porphyrin ring is 10.7 Å and 13.7 Å in PCN-223 and MOF-525, respectively. The well-defined and large spacing of metal cations became attractive for the development of spin-based qubits, and MOFs are now investigated for such applications.[60–64] Cu@PCN-224 has been identified as a suitable qubits-network candidate with copper(II) cations separated by ≈13 Å.[64] Herein, the ESR spectra of the non-metallated TCPP in both MOFs were similar to the spectrum of pure TCPP, with one sharp signal at $g \approx 2.003$ due to delocalized π electrons of the porphyrin, Figure S34.[65] In the spectrum of Cu@TCPP, only one asymmetric ESR line corresponding to copper(II) species with $g_{\perp} \approx 2.06$ is visible (Figure 5a) due to numerous spin-spin interactions in Cu@TCPP structure. Contrary to the spectrum of Cu@TCPP, both the TCPP signal at $g \approx 2.003$ and the hyperfine copper lines are resolved for both MOFs due to efficient separation of paramagnetic centers (Figures 5b and 5c).[65–67] Furthermore, ESR spectrum for Cu@MOF-525 shows additional, rarely observed structure – nine narrow lines in the first derivation (Figure 5b, inset), assigned to the interaction of copper having an electron spin S=1/2 with four nitrogen nucleus spins I=1 from TCPP coordinated planar to copper ion.[68] The occurrence of such superhyperfine interaction in Cu@MOF-525 stems from a large distance between the copper cations included in the *ftw* architecture and the essentially complete absence of their spin-spin interactions.[68,69] This behavior is not limited to copper, similar results are evident for polymorphs with Fe- or Mn@TCPP linkers (Figures S35b and S36).

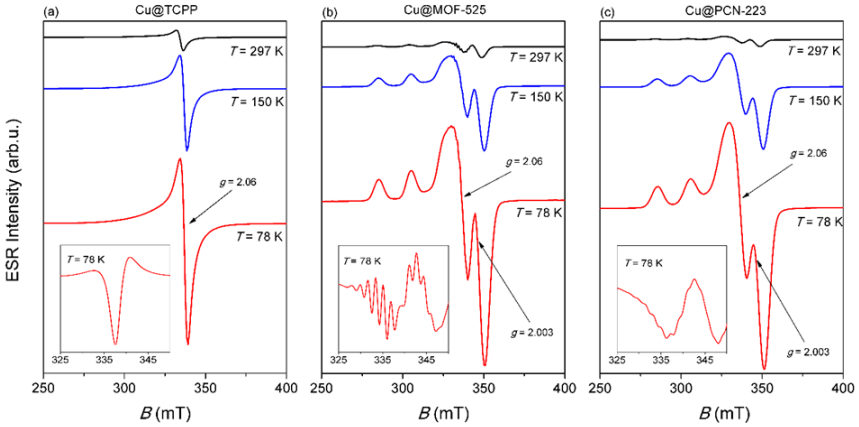

Figure 5. Comparison of ESR spectra for a) Cu@TCPP, b) Cu@MOF-525, and c) Cu@PCN-223. Insets show the first derivation of ESR spectra, i.e., the second derivation of the absorption spectra at 78 K.

In summary, we demonstrate how mechanochemistry can be used for a high-yielding, rapid, and selective synthesis of *ftw*-MOF-525 and *shp*-PCN-223 MOFs polymorphs. The control over the final product is achieved by the judicious use of the liquid additive and the zirconium precursor. *In situ* PXRD monitoring reveals that under most conditions explored herein the reaction proceeds directly to the specific product. However, LAG(MeOH) with the Zr_{12}-acetate precursor induces the formation of MOF-525 intermediate, which rapidly transforms into PCN-223, highlighting the importance of plastic deformations and introduced defects during the mechanochemical Zr-MOF nucleation. The different topologies mirror on the ESR spectra of paramagnetic centers in TCPP, based on their effective spatial isolation and varied geometry of TCPP. The results presented here show how the inclusion of paramagnetic cation into a porphyrin linker, combined with the polymorphism, stability, and well-defined architectures of polymorphic Zr-MOF supports may broaden the applicability of these important MOFs towards non-conventional magnetic materials, such as porous molecular spin qubits.[30]

ASSOCIATED CONTENT

Supporting Information

The Supporting Information is available free of charge on the ACS Publications website. Experimental details, computational details, PXRD data, FTIR spectra, details of porosity measurements, TGA data, ESR data (PDF).

AUTHOR INFORMATION

Corresponding Author

krunoslav.uzarevic@irb.hr

Notes

The authors declare no competing financial interests.

ACKNOWLEDGMENT

The authors are thankful to Ivan Halasz for help with the MOF-525 structure optimization, Stipe Lukin for help with graphical materials, and the reviewers for their comments that strongly affected the revised work. The research was supported by the Croatian Science Foundation under the projects 4744 and 3168. K.U., B.K., and T.F. acknowledge support from the European Social Fund and the Croatian Science Foundation (PZS-2019-02-4129). O.K.F. gratefully acknowledges support from the Defense Threat Reduction Agency (HDTRA1-19-1-0007). T.F. acknowledges the support of NSERC (RGPIN-2017-06467, STPGP 521582-18, and RGPAS 507837-17). The authors would like to acknowledge networking support by the COST Action CA18112 - Mechanochemistry for Sustainable Industry (www.mechsustind.eu) supported by COST (European Cooperation in Science and Technology, www.cost.eu).

REFERENCES

(1) Getman, R. B.; Bae, Y.-S.; Wilmer, C. E.; Snurr, R. Q. Review and Analysis of Molecular Simulations of Methane, Hydrogen, and Acetylene Storage in Metal–Organic Frameworks. *Chem. Rev.* **2012**, *112* (2), 703–723. https://doi.org/10.1021/cr200217c.

(2) Suh, M. P.; Park, H. J.; Prasad, T. K.; Lim, D.-W. Hydrogen Storage in Metal–Organic Frameworks. *Chem. Rev.* **2012**, *112* (2), 782–835. https://doi.org/10.1021/cr200274s.

(3) Sumida, K.; Rogow, D. L.; Mason, J. A.; McDonald, T. M.; Bloch, E. D.; Herm, Z. R.; Bae, T.-H.; Long, J. R. Carbon Dioxide Capture in Metal–Organic Frameworks. *Chem. Rev.* **2012**, *112* (2), 724–781. https://doi.org/10.1021/cr2003272.

(4) Li, J.-R.; Kuppler, R. J.; Zhou, H.-C. Selective Gas Adsorption and Separation in Metal–Organic Frameworks. *Chem. Soc. Rev.* **2009**, *38* (5), 1477–1504. https://doi.org/10.1039/b802426j.

(5) Li, J.; Sculley, J.; Zhou, H. Metal–Organic Frameworks for Separations. *Chem. Rev.* **2012**, *112* (2), 869–932. https://doi.org/10.1021/cr200190s.

(6) Lee, J.; Farha, O. K.; Roberts, J.; Scheidt, K. A.; Nguyen, S. T.; Hupp, J. T. Metal–Organic Framework Materials as Catalysts. *Chem. Soc. Rev.* **2009**, *38* (5), 1450. https://doi.org/10.1039/b807080f.

(7) Hasegawa, S.; Horike, S.; Matsuda, R.; Furukawa, S.; Mochizuki, K.; Kinoshita, Y.; Kitagawa, S. Three-Dimensional Porous Coordination Polymer Functionalized with Amide Groups Based on Tridentate Ligand: Selective Sorption and Catalysis. *J. Am. Chem. Soc.* **2007**, *129* (9), 2607–2614. https://doi.org/10.1021/ja067374y.

(8) Wang, C.; Liu, D.; Lin, W. Metal–Organic Frameworks as A Tunable Platform for Designing Functional Molecular Materials. *J. Am. Chem. Soc.* **2013**, *135* (36), 13222–13234. https://doi.org/10.1021/ja308229p.

(9) Zhang, T.; Lin, W. Metal–Organic Frameworks for Artificial Photosynthesis and Photocatalysis. *Chem. Soc. Rev.* **2014**, *43* (16), 5982–5993. https://doi.org/10.1039/C4CS00103F.

(10) Fateeva, A.; Chater, P. A.; Ireland, C. P.; Tahir, A. A.; Khimyak, Y. Z.; Wiper, P. V.; Darwent, J. R.; Rosseinsky, M. J. A Water-Stable Porphyrin-Based Metal-Organic Framework Active for Visible-Light Photocatalysis. *Angew. Chemie Int. Ed.* **2012**, *51* (30), 7440–7444. https://doi.org/10.1002/anie.201202471.

(11) Mondloch, J. E.; Katz, M. J.; Isley III, W. C.; Ghosh, P.; Liao, P.; Bury, W.; Wagner, G. W.; Hall, M. G.; DeCoste, J. B.; Peterson, G. W.; Snurr, R. Q.; Cramer, C. J.; Hupp, J. T.; Farha, O. K. Destruction of Chemical Warfare Agents Using Metal–Organic Frameworks. *Nat. Mater.* **2015**, *14* (5), 512–516. https://doi.org/10.1038/nmat4238.

(12) Cavka, J. H.; Jakobsen, S.; Olsbye, U.; Guillou, N.; Lamberti, C.; Bordiga, S.; Lillerud, K. P. A New Zirconium Inorganic Building Brick Forming Metal Organic Frameworks with Exceptional Stability. *J. Am. Chem. Soc.* **2008**, *130* (42), 13850–13851. https://doi.org/10.1021/ja8057953.

(13) Howarth, A. J.; Liu, Y.; Li, P.; Li, Z.; Wang, T. C.; Hupp, J. T.; Farha, O. K. Chemical, Thermal and Mechanical Stabilities of Metal–Organic Frameworks. *Nat. Rev. Mater.* **2016**, *1* (3), 15018. https://doi.org/10.1038/natrevmats.2015.18.

(14) Chen, Z.; Hanna, S. L.; Redfern, L. R.; Alezi, D.; Islamoglu, T.; Farha, O. K. Reticular Chemistry in the Rational Synthesis of Functional Zirconium Cluster-Based MOFs. *Coord. Chem. Rev.* **2019**, *386*, 32–49. https://doi.org/10.1016/j.ccr.2019.01.017.

(15) Deria, P.; Gómez-Gualdrón, D. A.; Hod, I.; Snurr, R. Q.; Hupp, J. T.; Farha, O. K. Framework-Topology-Dependent Catalytic Activity of Zirconium-Based (Porphinato)Zinc(II) MOFs. *J. Am. Chem. Soc.* **2016**, *138* (43), 14449–14457. https://doi.org/10.1021/jacs.6b09113.

(16) Feng, D.; Gu, Z.-Y.; Chen, Y.-P.; Park, J.; Wei, Z.; Sun, Y.; Bosch, M.; Yuan, S.; Zhou, H.-C. A Highly Stable Porphyrinic Zirconium Metal–Organic Framework with Shp-a Topology. *J. Am. Chem. Soc.* **2014**, *136* (51), 17714–17717. https://doi.org/10.1021/ja510525s.

(17) Jiang, H.-L.; Feng, D.; Wang, K.; Gu, Z.-Y.; Wei, Z.; Chen, Y.-P.; Zhou, H.-C. An Exceptionally Stable, Porphyrinic Zr Metal–Organic Framework Exhibiting PH-Dependent Fluorescence. *J. Am. Chem. Soc.* **2013**, *135* (37), 13934–13938. https://doi.org/10.1021/ja406844r.

(18) Nakagaki, S.; Ferreira, G.; Ucoski, G.; Dias de Freitas Castro, K. Chemical Reactions Catalyzed by Metalloporphyrin-Based Metal-Organic Frameworks. *Molecules* **2013**, *18* (6), 7279–7308. https://doi.org/10.3390/molecules18067279.

(19) Feng, D.; Gu, Z.-Y.; Li, J.-R.; Jiang, H.-L.; Wei, Z.; Zhou, H.-C. Zirconium-Metalloporphyrin PCN-222: Mesoporous Metal-Organic Frameworks with Ultrahigh Stability as Biomimetic Catalysts. *Angew. Chemie Int. Ed.* **2012**, *51* (41), 10307–10310. https://doi.org/10.1002/anie.201204475.

(20) Feng, D.; Chung, W.; Wei, Z.; Gu, Z.; Jiang, H.; Chen, Y.; Darensbourg, D. J.; Zhou, H. Construction of Ultrastable Porphyrin Zr Metal–Organic Frameworks through Linker Elimination. *J. Am. Chem. Soc.* **2013**, *135* (45), 17105–17110. https://doi.org/10.1021/ja408084j.

(21) Morris, W.; Volosskiy, B.; Demir, S.; Gándara, F.; McGrier, P. L.; Furukawa, H.; Cascio, D.; Stoddart, J. F.; Yaghi, O. M. Synthesis, Structure, and Metalation of Two New Highly Porous Zirconium Metal–Organic Frameworks. *Inorg. Chem.* **2012**, *51* (12), 6443–6445. https://doi.org/10.1021/ic300825s.

(22) Chen, Y.; Hoang, T.; Ma, S. Biomimetic Catalysis of a Porous Iron-Based Metal–Metalloporphyrin Framework. *Inorg. Chem.* **2012**, *51* (23), 12600–12602. https://doi.org/10.1021/ic301923x.

(23) Gong, X.; Noh, H.; Gianneschi, N. C.; Farha, O. K. Interrogating Kinetic versus Thermodynamic Topologies of Metal–Organic Frameworks via Combined Transmission Electron Microscopy and X-Ray Diffraction Analysis. *J. Am. Chem. Soc.* **2019**, *141* (15), 6146–6151. https://doi.org/10.1021/jacs.9b01789.

(24) Kelty, M. L.; Morris, W.; Gallagher, A. T.; Anderson, J. S.; Brown, K. A.; Mirkin, C. A.; Harris, T. D. High-Throughput Synthesis and Characterization of Nanocrystalline Porphyrinic Zirconium Metal–Organic Frameworks. *Chem. Commun.* **2016**, *52* (50), 7854–7857. https://doi.org/10.1039/C6CC03264H.

(25) Lyu, J.; Zhang, X.; Otake, K. I.; Wang, X.; Li, P.; Li, Z.; Chen, Z.; Zhang, Y.; Wasson, M. C.; Yang, Y.; Bai, P.; Guo, X.; Islamoglu, T.; Farha, O. K. Topology and Porosity Control of Metal-Organic Frameworks through Linker Functionalization. *Chem. Sci.* **2019**, *10* (4), 1186–1192. https://doi.org/10.1039/c8sc04220a.

(26) Shaikh, S. M.; Usov, P. M.; Zhu, J.; Cai, M.; Alatis, J.; Morris, A. J. Synthesis and Defect Characterization of Phase-Pure Zr-MOFs Based on Meso-Tetracarboxyphenylporphyrin. *Inorg. Chem.* **2019**, *58* (8), 5145–5153. https://doi.org/10.1021/acs.inorgchem.9b00200.

(27) Do, J.-L.; Friščić, T. Chemistry 2.0: Developing a New, Solvent-Free System of Chemical Synthesis Based on Mechanochemistry. *Synlett* **2017**, *28* (16), 2066–2092. https://doi.org/10.1055/s-0036-1590854.

(28) Crawford, D.; Casaban, J.; Haydon, R.; Giri, N.; McNally, T.; James, S. L. Synthesis by Extrusion: Continuous, Large-Scale Preparation of MOFs Using Little or No Solvent. *Chem. Sci.* **2015**, *6* (3), 1645–1649. https://doi.org/10.1039/C4SC03217A.

(29) Užarević, K.; Wang, T. C.; Moon, S.-Y.; Fidelli, A. M.; Hupp, J. T.; Farha, O. K.; Friščić, T. Mechanochemical and Solvent-Free Assembly of Zirconium-Based Metal–Organic Frameworks. *Chem. Commun.* **2016**, *52* (10), 2133–2136. https://doi.org/10.1039/C5CC08972G.

(30) Crawford, D. E. Extrusion – Back to the Future: Using an Established Technique to Reform Automated Chemical Synthesis. *Beilstein J. Org. Chem.* **2017**, *13*, 65–75. https://doi.org/10.3762/bjoc.13.9.

(31) Klimakow, M.; Klobes, P.; Thünemann, A. F.; Rademann, K.; Emmerling, F. Mechanochemical Synthesis of Metal−Organic Frameworks: A Fast and Facile Approach toward Quantitative Yields and High Specific Surface Areas. *Chem. Mater.* **2010**, *22* (18), 5216–5221. https://doi.org/10.1021/cm1012119.

(32) Julien, P. A.; Mottillo, C.; Friščić, T. Metal–Organic Frameworks Meet Scalable and Sustainable Synthesis. *Green Chem.* **2017**, *19* (12), 2729–2747. https://doi.org/10.1039/C7GC01078H.

(33) Katsenis, A. D.; Puškarić, A.; Štrukil, V.; Mottillo, C.; Julien, P. A.; Užarević, K.; Pham, M.-H.; Do, T.-O.; Kimber, S. A. J.; Lazić, P.; Magdysyuk, O.; Dinnebier, R. E.; Halasz, I.; Friščić, T. In Situ X-Ray Diffraction Monitoring of a Mechanochemical Reaction Reveals a Unique Topology Metal-Organic Framework. *Nat. Commun.* **2015**, *6* (1), 6662. https://doi.org/10.1038/ncomms7662.

(34) Halasz, I.; Kimber, S. A. J.; Beldon, P. J.; Belenguer, A. M.; Adams, F.; Honkimäki, V.; Nightingale, R. C.; Dinnebier, R. E.; Friščić, T. In Situ and Real-Time Monitoring of Mechanochemical Milling Reactions Using Synchrotron X-Ray Diffraction. *Nat. Protoc.* **2013**, *8* (9), 1718–1729. https://doi.org/10.1038/nprot.2013.100.

(35) Užarević, K.; Halasz, I.; Friščić, T. Real-Time and In Situ Monitoring of Mechanochemical Reactions: A New Playground for All Chemists. *J. Phys. Chem. Lett.* **2015**, *6* (20), 4129–4140. https://doi.org/10.1021/acs.jpclett.5b01837.

(36) Julien, P. A.; Užarević, K.; Katsenis, A. D.; Kimber, S. A. J.; Wang, T.; Farha, O. K.; Zhang, Y.; Casaban, J.; Germann, L. S.; Etter, M.; Dinnebier R. E.; James, S. L.; Halasz, I.; Friščić, T In Situ Monitoring and Mechanism of the Mechanochemical Formation of a Microporous MOF-74 Framework. *J. Am. Chem. Soc.* **2016**, *138* (9), 2929–2932. https://doi.org/10.1021/jacs.5b13038.

(37) Cindro, N.; Tireli, M.; Karadeniz, B.; Mrla, T.; Užarević, K. Investigations of Thermally Controlled Mechanochemical Milling Reactions. *ACS Sustain. Chem. Eng.* **2019**, *7* (19), 16301–16309. https://doi.org/10.1021/acssuschemeng.9b03319.

(38) Ayoub, G.; Karadeniz, B.; Howarth, A. J.; Farha, O. K.; Đilović, I.; Germann, L. S.; Dinnebier, R. E.; Užarević, K.; Friščić, T. Rational Synthesis of Mixed-Metal Microporous Metal–Organic Frameworks with Controlled Composition Using Mechanochemistry. *Chem. Mater.* **2019**, *31* (15), 5494–5501. https://doi.org/10.1021/acs.chemmater.9b01068.

(39) Prochowicz, D.; Sokołowski, K.; Justyniak, I.; Kornowicz, A.; Fairen-Jimenez, D.; Friščić, T.; Lewiński, J. A Mechanochemical Strategy for IRMOF Assembly Based on Pre-Designed Oxo-Zinc Precursors. *Chem. Commun.* **2015**, *51* (19), 4032–4035. https://doi.org/10.1039/C4CC09917F.

(40) Stolar, T.; Batzdorf, L.; Lukin, S.; Žilić, D.; Motillo, C.; Friščić, T.; Emmerling, F.; Halasz, I.; Užarević, K. In Situ Monitoring of the Mechanosynthesis of the Archetypal Metal-Organic Framework HKUST-1: Effect of Liquid Additives on the Milling Reactivity. *Inorg. Chem.* **2017**, *56* (11), 6599–6608. https://doi.org/10.1021/acs.inorgchem.7b00707.

(41) Arhangelskis, M.; Katsenis, A. D.; Novendra, N.; Akimbekov, Z.; Gandrath, D.; Marrett, J. M.; Ayoub, G.; Morris, A. J.; Farha, O. K.; Friščić, T.; et al. Theoretical Prediction and Experimental

Evaluation of Topological Landscape and Thermodynamic Stability of a Fluorinated Zeolitic Imidazolate Framework. *Chem. Mater.* **2019**, *31* (10), 3777–3783. https://doi.org/10.1021/acs.chemmater.9b00994.

(42) Karadeniz, B.; Howarth, A. J.; Stolar, T.; Islamoglu, T.; Dejanović, I.; Tireli, M.; Wasson, M. C.; Moon, S.-Y.; Farha, O. K.; Friščić, T.; Užarević, K. Benign by Design: Green and Scalable Synthesis of Zirconium UiO-Metal–Organic Frameworks by Water-Assisted Mechanochemistry. *ACS Sustain. Chem. Eng.* **2018**, *6* (11), 15841–15849. https://doi.org/10.1021/acssuschemeng.8b04458.

(43) Fidelli, A. M.; Karadeniz, B.; Howarth, A. J.; Huskić, I.; Germann, L. S.; Halasz, I.; Etter, M.; Moon, S.-Y.; Dinnebier, R. E.; Stilinović, V.; et al. Green and Rapid Mechanosynthesis of High-Porosity NU- and UiO-Type Metal–Organic Frameworks. *Chem. Commun.* **2018**, *54* (51), 6999–7002. https://doi.org/10.1039/C8CC03189D.

(44) Huang, Y.-H.; Lo, W.-S.; Kuo, Y.-W.; Chen, W.-J.; Lin, C.-H.; Shieh, F.-K. Green and Rapid Synthesis of Zirconium Metal–Organic Frameworks via Mechanochemistry: UiO-66 Analog Nanocrystals Obtained in One Hundred Seconds. *Chem. Commun.* **2017**, *53* (43), 5818–5821. https://doi.org/10.1039/C7CC03105J.

(45) Lukin, S.; Stolar, T.; Tireli, M.; Blanco, M. V.; Babić, D.; Friščić, T.; Užarević, K.; Halasz, I. Tandem In Situ Monitoring for Quantitative Assessment of Mechanochemical Reactions Involving Structurally Unknown Phases. *Chem. Eur. J.* **2017**, *23* (56), 13941–13949. https://doi.org/10.1002/chem.201702489.

(46) Hasa, D.; Miniussi, E.; Jones, W. Mechanochemical Synthesis of Multicomponent Crystals: One Liquid for One Polymorph? A Myth to Dispel. *Cryst. Growth Des.* **2016**, *16* (8), 4582–4588. https://doi.org/10.1021/acs.cgd.6b00682.

(47) Užarević, K.; Rubčić, M.; Đilović, I.; Kokan, Z.; Matković-Čalogović, D.; Cindrić, M. Concomitant Conformational Polymorphism: Mechanochemical Reactivity and Phase Relationships in the (Methanol) Cis -Dioxo(N -Salicylidene-2-Amino-3-Hydroxypyridine)Molybdenum(VI) Trimorph. *Cryst. Growth Des.* **2009**, *9* (12), 5327–5333. https://doi.org/10.1021/cg900824n.

(48) Friščić, T.; Reid, D. G.; Halasz, I.; Stein, R. S.; Dinnebier, R. E.; Duer, M. J. Ion- and Liquid-Assisted Grinding: Improved Mechanochemical Synthesis of Metal-Organic Frameworks Reveals Salt Inclusion and Anion Templating. *Angew. Chemie Int. Ed.* **2010**, *49* (4), 712–715. https://doi.org/10.1002/anie.200906583.

(49) Mottillo, C.; Friščić, T. Advances in Solid-State Transformations of Coordination Bonds: From the Ball Mill to the Aging Chamber. *Molecules* **2017**, *22* (1), 144. https://doi.org/10.3390/molecules22010144.

(50) Akimbekov, Z.; Katsenis, A. D.; Nagabhushana, G. P.; Ayoub, G.; Arhangelskis, M.; Morris, A. J.; Friščić, T.; Navrotsky, A. Experimental and Theoretical Evaluation of the Stability of True MOF Polymorphs Explains Their Mechanochemical Interconversions. *J. Am. Chem. Soc.* **2017**, *139* (23), 7952–7957. https://doi.org/10.1021/jacs.7b03144.

(51) Friščić, T.; Childs, S. L.; Rizvi, S. A. A.; Jones, W. The Role of Solvent in Mechanochemical and Sonochemical Cocrystal Formation: A Solubility-Based Approach for Predicting Cocrystallisation Outcome. *CrystEngComm* **2009**, *11* (3), 418–426. https://doi.org/10.1039/B815174A.

(52) Friščić, T.; Halasz, I.; Beldon, P. J.; Belenguer, A. M.; Adams, F.; Kimber, S. A. J.; Honkimäki, V.; Dinnebier, R. E. Real-Time and in Situ Monitoring of Mechanochemical Milling Reactions. *Nat. Chem.* **2013**, *5* (1), 66–73. https://doi.org/10.1038/nchem.1505.

(53) Hutchings, B. P.; Crawford, D. E.; Gao, L.; Hu, P.; James, S. L. Feedback Kinetics in Mechanochemistry: The Importance of Cohesive States. *Angew. Chemie Int. Ed.* **2017**, *56*, 15252–15256. https://doi.org/10.1002/anie.201706723.

(54) Pawley, G. Unit-Cell Refinement from Powder Diffraction Scans. *J. Appl. Crystallogr.* **1981**, *14* (6), 357–361.

(55) Our attempts to confirm the relative stability between two MOFs by standard slurry technique performed in DMF were not successful. The starting reaction mixture containing both MOFs remained unchanged after eight days of stirring at 80 °C (Figure S17).

(56) Based on $[Zr_6O_4(OH)_4(CuC_{48}N_4O_8H_{24})_3]$ unit containing 273 atoms, molar mass = 3222 g/Mol.

(57) Perdew, J. P.; Burke, K.; Ernzerhof, M. Generalized Gradient Approximation Made Simple. *Phys. Rev. Lett.* **1996**, *77* (18), 3865–3868. https://doi.org/10.1103/PhysRevLett.77.3865.

(58) Grimme, S.; Antony, J.; Ehrlich, S.; Krieg, H. A Consistent and Accurate Ab Initio Parametrization of Density Functional Dispersion Correction (DFT-D) for the 94 Elements H-Pu. *J. Chem. Phys.* **2010**, *132* (15), 154104. https://doi.org/10.1063/1.3382344.

(59) Grimme, S.; Ehrlich, S.; Goerigk, L. Effect of the Damping Function in Dispersion Corrected Density Functional Theory. *J. Comput. Chem.* **2011**, *32* (7), 1456–1465. https://doi.org/10.1002/jcc.21759.

(60) Mínguez Espallargas, G.; Coronado, E. Magnetic Functionalities in MOFs: From the Framework to the Pore. *Chem. Soc. Rev.* **2018**, *47* (2), 533–557. https://doi.org/10.1039/C7CS00653E.

(61) Gaita-Ariño, A.; Luis, F.; Hill, S.; Coronado, E. Molecular Spins for Quantum Computation. *Nat. Chem.* **2019**, *11* (4), 301–309. https://doi.org/10.1038/s41557-019-0232-y.

(62) Graham, M. J.; Zadrozny, J. M.; Fataftah, M. S.; Freedman, D. E. Forging Solid-State Qubit Design Principles in a Molecular Furnace. *Chem. Mater.* **2017**, *29* (5), 1885–1897. https://doi.org/10.1021/acs.chemmater.6b05433.

(63) Yamabayashi, T.; Atzori, M.; Tesi, L.; Cosquer, G.; Santanni, F.; Boulon, M.-E.; Morra, E.; Benci, S.; Torre, R.; Chiesa, M.; et al. Scaling Up Electronic Spin Qubits into a Three-Dimensional Metal–Organic Framework. *J. Am. Chem. Soc.* **2018**, *140* (38), 12090–12101. https://doi.org/10.1021/jacs.8b06733.

(64) Yu, C.-J.; Krzyaniak, M. D.; Fataftah, M. S.; Wasielewski, M. R.; Freedman, D. E. A Concentrated Array of Copper Porphyrin Candidate Qubits. *Chem. Sci.* **2019**, *10* (6), 1702–1708. https://doi.org/10.1039/C8SC04435J.

(65) Feng, D.; Jiang, H.-L.; Chen, Y.-P.; Gu, Z.-Y.; Wei, Z.; Zhou, H.-C. Metal–Organic Frameworks Based on Previously Unknown Zr 8 /Hf 8 Cubic Clusters. *Inorg. Chem.* **2013**, *52* (21), 12661–12667. https://doi.org/10.1021/ic4018536.

(66) Zheng, W.; Shan, N.; Yu, L.; Wang, X. UV–Visible, Fluorescence and EPR Properties of Porphyrins and Metalloporphyrins. *Dye. Pigment.* **2008**, *77* (1), 153–157. https://doi.org/10.1016/j.dyepig.2007.04.007.

(67) Diaz-Uribe, C. E.; Vallejo, W.; Reales, Y.; Correa, P. Degradación de Fenol Por Proceso Haber-Weiss Fotoinducido Por Luz Visible Con Tetracarboxifenilporfirina de Cobre (Ii) Anclada Al Dióxido de Titanio. *Prospectiva* **2015**, *13* (2), 47. https://doi.org/10.15665/rp.v13i2.486.

(68) Fidalgo-Marijuan, A.; Barandika, G.; Bazán, B.; Urtiaga, M. K.; Larrea, E. S.; Iglesias, M.; Lezama, L.; Arriortua, M. I. Heterogeneous Catalytic Properties of Unprecedented μ-O-[FeTCPP] 2 Dimers (H 2 TCPP = Meso-Tetra(4-Carboxyphenyl)Porphyrin): An Unusual Superhyperfine EPR Structure. *Dalt. Trans.* **2015**, *44* (1), 213–222. https://doi.org/10.1039/C4DT02250E.

(69) Stubbs, A. W.; Braglia, L.; Borfecchia, E.; Meyer, R. J.; Román-Leshkov, Y.; Lamberti, C.; Dincă, M. Selective Catalytic Olefin Epoxidation with Mn II -Exchanged MOF-5. *ACS Catal.* **2018**, *8* (1), 596–601. https://doi.org/10.1021/acscatal.7b02946.